Nanometer scale patterning using focused ion beam milling

D. Petit and C. C. Faulkner
Nanoscale Magnetics Group, Department of Physics, University of Durham, South Road, Durham DH1 3LE, United Kingdom

S. Johnstone
Centre for Electronic Systems, School of Engineering, University of Durham, Durham, United Kingdom

D. Wood
Microsystems Technology Group, School of Engineering, University of Durham, Durham, United Kingdom

R. P. Cowburn
Nanoscale Magnetics Group, Department of Physics, University of Durham, South Road, Durham DH1 3LE, United Kingdom

(Received 4 October 2004; accepted 15 November 2004; published online 7 January 2005)

We report on the performance of focused ion beam (FIB) milling in order to produce nanometer scale devices. Resolution issues have been systematically studied as a function of emission current and working distance, by imaging single pixel lines FIB milled into thin bismuth films deposited on oxidized silicon. The ion beam profile has been measured, and by carefully optimizing the milling conditions, 40 nm Hall probe sensors have been fabricated. © *2005 American Institute of Physics.* [DOI: 10.1063/1.1844431]

FIB milling has proven to be a very powerful tool to fabricate nanoscale structures. It is used in the development of nanoelectronics,[1] nanoscale probe recording,[2] and magnetoelectronics,[3] or for high resolution modification of MFM tips.[4] We have recently demonstrated the ability of the FIB technique to fabricate 50 nm wide Hall effect sensors.[5] The main advantage of FIB is that it is a very rapid, dry technique, as compared to electron beam lithography for instance. FIB patterning consists of exposing the target to a high energy focused ion beam in order to sputter away the target material. The resolution which can be reached using this technique first depends on the selected aperture size which defines the ion current[2] and on the target material (the lateral damage and sputtering yield induced by the ion beam depend on the target composition, as can be estimated from TRIM calculations).[6] However, for a given ion aperture and target we show that it is possible to greatly improve the resolution offered by standard commercial systems by reducing the emission current (EC) and working distance (WD).

Measuring the focusing properties of an ion beam can be done by several ways, such as using a Faraday cup of known dimensions and a deconvolution procedure,[7] although the spatial resolution of this technique is limited, or by exposing a target to the ion beam and measuring the damage done to it.[8–10] We have chosen the second method: a 50 nm thick Bi film is first deposited by thermal evaporation (1 Å/s, 10^{-6} mbars) on thermally oxidized silicon substrates; FIB milling is then performed using the 1 pA aperture of an FEI 200xP® FIB workstation (Ga^+ LMIS operated at 30 keV) and resolution tests are carried out by milling single pixel lines. For milling these 1D structures, the ion beam is rastered along a line (dwell time 1 ms, overlap 50%, magnification ×200k), as many times as is needed to achieve the required dose. Figure 1 shows two SEM pictures of these structures. The widths of the lines have been measured using image analysis software: the gray level value has been averaged over the height of the picture, and the width at half maximum has been retained. Bi has originally been used because we are interested in fabricating nanoscale Hall sensors.[5] Additionally, however, the large difference between the atomic number of Bi and the mean atomic number of SiO_2 causes the SEM contrast between the cleared substrate and the Bi film to be excellent.

In our FIB system, the ion beam is produced by extracting ions from a LMIS by applying a high voltage relative to the source to a nearby electrode. The total ion current extracted from the source is the EC, and is of the order of few μA. Ion beams produced at ever higher EC are known to be composed of an ever increasing proportion of dimers, trimers, and charged clusters.[11] At low EC, reducing the EC reduces the width of the energy distribution of the beam,[11,12] and therefore improves the performance of a given source by reducing the effect of chromatic aberration in the optical system. We have measured the effect of reducing the EC below the default value set for basic FIB use (2.2 μA), and have indeed found that reducing it to 1 μA improves the resolution by 20%. The rest of the experiments have therefore been performed using this low value.

FIB systems are known to have a large depth of focus,[13] and this property is used implicitly in commercial systems where all the settings for the focusing lenses are optimized for a particular stage height, called the eucentric height. It will be referred to thereafter as normal working distance (NWD). However, reducing the WD should increase the resolution;[11] we have therefore estimated the beam profile at NWD, NWD+4 mm and +8 mm, by measuring the variation of the width of lines as a function of dose. The areal dose is defined as $d_S = I \times t/S$, where I is the ion current (1 pA), t is

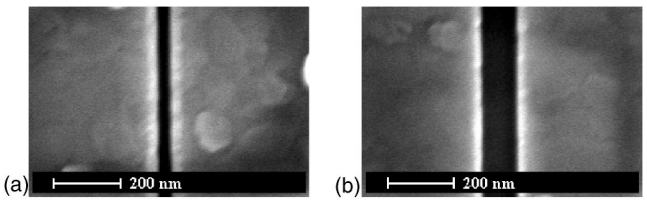

FIG. 1. SEM images of lines milled in 50 nm Bi deposited on SiO_2.

the exposure time, and S is the area of the exposed surface. The milling rate of Ga^+ 30 keV into Bi has been estimated by performing standard AFM depth measurements and the threshold dose d_0 necessary to mill through our 50 nm thick film has been measured at 32.6 ± 3 C m^{-2}. Ion beams are known to have a Gaussian distribution,[7] or Gaussian with exponential tails.[8,9] Such a dose profile is written as $D(x) = d_L \times d_i(x)$ ($d_L = I \times t/L$ is the line dose, L is the length of the line), with

$$d_1(x) = \frac{\alpha}{\sqrt{2\pi}\sigma} \exp\left(-\frac{x^2}{2\sigma^2}\right) \text{ for } |x| < x_0, \tag{1}$$

$$d_2(x) = b \exp\left(-\frac{|x|}{\beta}\right) \text{ for } \quad |x| > x_0. \tag{2}$$

The measured width divided by two is then the value x such that $D(x) = d_0$, so that

$$\frac{d_i(x)}{d_0} = \frac{d_i\left(\frac{w}{2}\right)}{d_0} = \frac{1}{d_L}, \quad i = 1,2. \tag{3}$$

Figure 2(a) (circles) shows the width vs dose data at NWD $+8$ mm: $1/d_L$ is plotted as a function of $x = w/2$, and the data have been made symmetric with respect to the center of the beam. According to Eq. (3), this plot is a direct representation of the beam profile $d_i(x)/d_0$. The central part of the data has been fitted using Eqs. (1) and (3), with α/d_0 and σ as free parameters, and the external part of the data have been fitted using Eqs. (2) and (3) with b/d_0 and β as free parameters. An illustration of the result of the fit is shown Fig. 2(a) (solid lines). The values found for σ, β, and the ratio $R = \alpha/(b\sqrt{2\pi}\sigma)$ as a function of WD are shown Fig. 2(b). As the stage is raised, σ decreases, β increases, and R increases. In summary, the ion beam is sharper as the WD decreases.

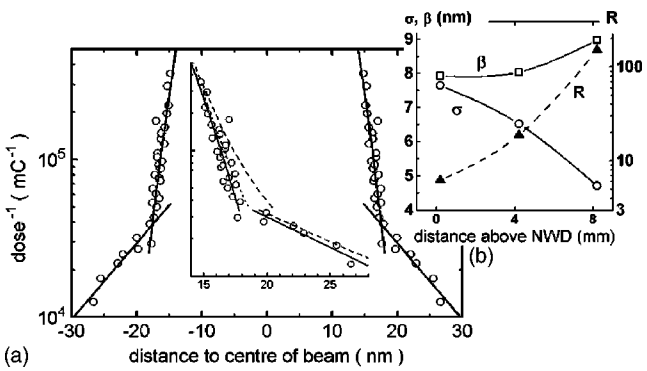

FIG. 2. (a) Inverse of the dose as a function of the half of the width at NWD+8 mm. Inset: zoom of the $x>0$ side of the data. (b) Parameters describing the beam profile as a function of WD.

The method we have used should be independent of the target material and thickness, as the target dependency should only affect the parameter d_0. However, this point has not been verified.

The mechanical and thermal stage drift has not been taken into account in the previous beam profile analysis. As we have used exposure times as long as 60 s, its effect can potentially be important, especially if the beam is sharp, as in that case broadening due to the distance traveled during exposure might dominate over the broadening due to the natural width of the beam. Stage drift rate measurements presented in Ref. 13 show that the longer the time elapsed since the last major stage movement, the smaller the drift. We have performed drift measurements on our system in the time range that is of interest for us, namely after up to 30 min after the last main stage movement. No clear trend could be observed with the time after last stage movement between 30 s and 30 min. The stage drift is isotropic and does not slow down with time in the time range investigated. The mean distance $\langle R \rangle$ the stage has moved during t can be modeled as a 2D random walk $\langle R \rangle = \sqrt{Kt}$. The diffusion coefficient $\sqrt{K}$ projected on one direction (only the drift in the x direction matters) has been measured at about 1.2 nm $s^{-1/2}$, and up to 2.4 nm $s^{-1/2}$. We have estimated the effect of the stage drift for the sharpest beam profile obtained for NWD $+8$ mm. In the presence of stage drift, Eq. (1) has to be slightly transformed, and the dose profile for a time T is

$$D(x) = \frac{I}{L}\frac{\alpha}{\sqrt{2\pi}\sigma}\int_0^T \exp\left(-\frac{\left(x-\sqrt{\frac{K}{2}t}\right)^2}{2\sigma^2}\right)dt. \tag{4}$$

We have numerically estimated the width of lines milled with a beam profile such as Eq. (4) with the parameters obtained at NWD+8 mm. The results are displayed in the inset of Fig. 2(a), where the experimental data are shown together with the fits obtained without drift, and the curves obtained when taking the stage drift into account: the dotted line has been obtained using $\sqrt{K} = 1.2$ nm $s^{-1/2}$, and the dashed lines using 2.4 nm $s^{-1/2}$. As can be seen on this graph, the scattering of the experimental data can be explained by the existence of this stage drift (the dashed line gives a statistical superior boundary value to the data). The calculated effect of the stage drift on the width of lines milled with the tails of the ion beam (high doses) is negligible, as can be seen by comparing the dashed line with the corresponding static fit of the experimental data. The analysis we have done without considering the stage drift has led us to a slight overestimation of the beam width, and this overestimation is greater as the beam is sharper, i.e., as the WD decreases. Taking the stage drift fully into account in the beam shape analysis would then lead to an even greater change in the parameter σ with the WD.

The shape of the beam profile, more than simply the width of milled lines, determines the ultimate size of features that can be patterned using FIB, by determining how close two lines can be brought together (remember FIB patterning consists in removing unwanted parts of the film in order to leave the desired structure). Figure 3 shows the dose profile

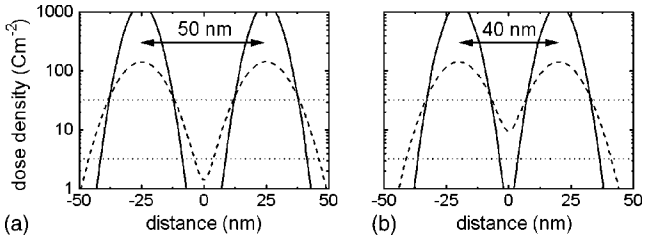

FIG. 3. Dose profile for 1 s exposure when the ion beam is positioned at two different points separated by l. (a) $l=40$ nm; (b) $l=50$ nm.

for 1 s exposure as a function of lateral position when the ion beam is positioned at two different points separated by a distance l, for NWD (dashed lines) and for 8 mm above NWD (solid lines), and for (a) $l=50$ nm, and (b) $l=40$ nm. The upper dotted line represents the dose threshold d_0, the lower one is $d_0/10$. For large enough l, the dose at the center position is negligible in both cases, but for $l=50$ nm (a), at NWD and NWD+8 mm, an 8 nm wide and 18 nm wide area is irradiated with a dose of less than $d_0/10$, respectively. As l decreases further, the center position is more and more irradiated, until the two milled lines eventually collapse for l small enough. For $l=40$ nm (b), at NWD, the central zone is irradiated with a dose sufficient to remove one third of the thickness of the film, whereas at NWD+8 mm, an 8 nm wide area has received a dose less than $d_0/10$. We have demonstrated[5] the ability of the FIB to pattern 50 nm wide, 70 nm thick Hall devices, by milling 4 lines at right angles with a gap at the center. The nanosensors in this paper had been fabricated using an ion current of 1 pA, an EC of 1 μA, and by placing the sample at NWD. None of the devices smaller than 50 nm were electrically viable, and this fact had been explained qualitatively by evoking a hypothetical Gaussian profile for the ion beam. We see here more quantitatively that at NWD, any attempt to decrease this distance in order to make the Hall sensor smaller, is causing the central part to be seriously irradiated, and therefore partly milled away, consequently less likely to sustain any electrical current. At NWD+8 mm, on the contrary, the same central irradiation dose is not attained for $l=40$ nm. Fabricating the Hall structures at this reduced WD should allow a further reduction of their sizes. We have indeed been able to fabricate 40 nm wide Hall probes which can sustain a current of a few tens of μA. Figure 4 shows a SEM image of one of these 40 nm wide, 50 nm thick Hall devices. Its Hall sensitivity R_H has been measured at 5×10^{-8} Ω mT^{-1} (30 μA driving current and $B_\perp=0.12$ T), its series resistance at 4 kΩ, and its transverse offset resistance, due to an unavoidable misalignment in the voltage pads at the center, at 26.6 Ω, consistent with the high specific resistivity of Bi in very small structures. The longitudinal and transverse $I-V$ curves (not shown here) under zero magnetic field have been found Ohmic.

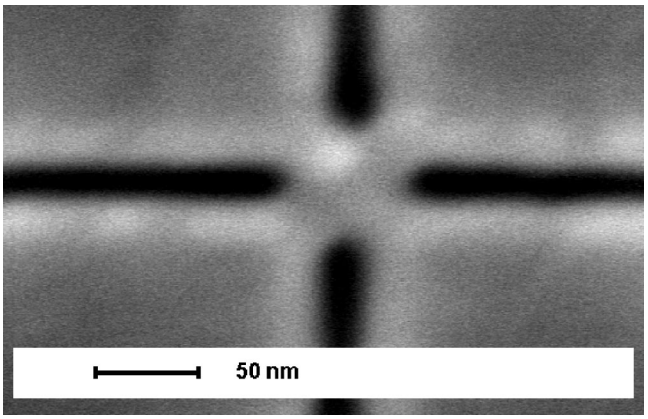

FIG. 4. SEM image of the central part of a 40 nm wide, 50 nm thick Bi Hall probe. The dark areas are the exposed SiO_2 substrate, the bright areas are the Bi film. The arms of the cross are oriented at 45°.

We have presented in this paper results concerning patterning resolution using a commercial FIB system. Single pixel lines have been milled on a 50 nm thick Bi film deposited on SiO_2 and the effect of changing FIB parameters such as the EC and the WD, has been studied by measuring their widths. The beam profile has been measured: it has an intense Gaussian central part, which deviates two to three orders of magnitude below the maximum value to exponential tails. Reducing the EC and the WD significantly improves the resolution, and the effect of the latter has been quantified by measuring the change in the beam shape parameters. By optimizing the fabrication conditions, we have fabricated 40 nm wide Hall sensors whose transport parameters are presented.

This work has been supported by UK EPSRC.

[1] U. Dötsch and A. D. Wieck, Nucl. Instrum. Methods Phys. Res. B **139**, 12 (1998).
[2] D. Litvinov and S. Khizroev, Nanotechnology **13**, 179 (2002).
[3] Gang Xiong, D. A. Allwood, M. D. Cooke, and R. P. Cowburn, Appl. Phys. Lett. **79**, 3461 (2001).
[4] L. Folks, M. E. Best, P. M. Rice, B. D. Terris, D. Weller, and J. N. Chapman, Appl. Phys. Lett. **76**, 909 (2000).
[5] D. Petit, D. Atkinson, S. Johnstone, D. Wood, and R. P. Cowburn, IEE Proc.: Sci., Meas. Technol. **151**, 127 (2004).
[6] J. Ziegler, J. P. Biersack, and U. Littmark, *The Stopping of Ions in Matter* (Pergamon, New York, 1985).
[7] C. E. Sosolik, A. C. Lavery, E. B. Dahl, and B. H. Cooper, Rev. Sci. Instrum. **71**, 3326 (2000).
[8] A. Lugstein, B. Basnar, G. Hobler, and E. Bertagnolli, J. Appl. Phys. **92**, 4037 (2002).
[9] R. L. Kubena and J. W. Ward, Appl. Phys. Lett. **51**, 1960 (1987).
[10] M. Komuro, T. Kanayama, H. Hiroshima, and H. Tanoue, Appl. Phys. Lett. **42**, 908 (1983).
[11] J. Orloff, Rev. Sci. Instrum. **64**, 1105 (1993).
[12] P. Marriott, Appl. Phys. A: Solids Surf. **A44**, 329 (1987).
[13] D. M. Longo, W. E. Benson, T. Chraska, and R. Hull, Appl. Phys. Lett. **78**, 981 (2001).